Journal of the Chinese Chemical Society, **1994**, *41*, 293-308

Invited Paper

Applications of Laser-enhanced Ionization in Analytical Chemistry*

King-Chuen Lin (林金全)
Department of Chemistry, National Taiwan University, Taipei, Taiwan, and Institute of Atomic and Molecular Sciences, Academia Sinica, P.O. Box 23-166, Taipei, Taiwan 10764, R.O.C.

Various applications of laser-enhanced ionization (LEI) in analytical chemistry are reviewed. This technique was applied to determine some physical quantities associated with a flame through development of an appropriate model. Determinations of flame temperature and atomization efficiency of an element in the flame are examples. As trace analysis is an important application of this technique, we compare the ion yield induced in a two-step LEI with that in a one-step LEI. The factors governing the ion enhancement via two-step excitation are examined in order to make efficient use of the two-step LEI apparatus. A novel technique was designed to couple flow-injection analysis to a conventional LEI device; in this manner, electrical interference, a severe problem inherent in LEI, was successfully removed.

INTRODUCTION

Laser-enhanced ionization (LEI) technique has been thoroughly developed to the point at which it has become a "textbook" analytical tool, which is very powerful especially in the trace analysis.[1-10] The principle of LEI involves using a tunable dye laser to promote the population of an analyte to its excited state, and then monitoring the resultant ion yield. According to the Boltzmann theory, the rate of collisional ionization of the excited analyte may be enhanced substantially over that of its ground state. Therefore, the detection limit achieved by the LEI technique can feasibly reach a sub-pg/mL region for most trace elements.[1-8]

Recent exploration indicates that this technique is as capable as other spectrometric methods in many fields. For instance, the LEI technique has been successfully employed to measure the ion lifetime,[11] the free atoms released,[12] and the atomization efficiency in a flame,[13] to diagnose the ion mobility, diffusion coefficients and temperature of a flame,[14-16] to determine the structures of atomic, molecular and free-radical species,[17-20] and to be coupled to a chromatograph as a detector.[10,21]

We confine the scope of this review to four varied applications of LEI in analytical chemistry, that have been conducted in our laboratory. We applied the LEI technique to determine some physical quantities associated with a flame through an appropriate model development. Determinations of flame temperature and atomization efficiency are selected for demonstration.[13,16] As trace anaysis is an important application of this technique, we compare the ion yield induced in a two-step LEI with that in a one-step LEI. The factors governing the ion enhancement via two-step optical excitation are examined in order to make efficient use of the two-step LEI apparatus.[6] A novel technique was designed to couple flow-injection analysis (FIA) to the conventional LEI device;[22] in this manner, electrical interference caused by a mixture with easily ionized matrices, which is a severe problem inherent in LEI, was successfully diminished.

EXPERIMENTAL SECTION

The basic LEI apparatus, shown in Fig. 1, is composed of a flame burner assembly, a pair of metal electrodes as collector of charged particles and a laser source of radiation; as details are presented previously,[6,13,16,23,24] and reported elsewhere,[1-5,9] only a brief account appears here.

To generate atomic elements in a flame, we used a burner head, a commercial assembly with a slot 100 mm × 0.5 mm, coupled with an interlocked system for gas control in which acetylene (0.5 L/min) and air (12.5 L/min) were premixed before reaching the burner head. The flame temperature was about 2500 K.[16]

A tunable dye laser pumped by a 10 Hz, frequency-doubled Nd:YAG laser was employed as source of radiation. The output wavelength could be tuned with the use of an appropriate laser dye. When UV radiation was required, the output frequency was doubled in a KDP crystal. The dye la-

*Delivered as an invited lecture in the 1993 International Conference of Analytical Chemistry at Sun Yat-Sen University, Kaohsiung, Oct. 13-16.

ser had pulse duration 5-8 ns, and a linewidth ~ 1 cm^{-1}. Its output power was monitored by a surface-absorbing disc calorimeter throughout the experiment. The laser beam was directed longitudinally through the flame at 7.5 ± 0.5 mm above the burner head. In the conduct of a two-step LEI experiment, the additional tunable laser beam, pumped simultaneously by the same Nd:YAG laser, was directed from the side opposite to the first laser beam. The two beams overlapped temporally and spatially above the center of the burner head. The unfocused laser beams involved were collimated through an aperture of diameter 2.5 ± 0.5 mm to allow for a homogeneous photon fluence impinging through the flame. In this manner scattered light was eliminated, so that the ionized amount of sample atoms probably caused by it could be neglected.[25]

The resulting LEI ions were collected with a pair of voltage-biased electrodes along the flame. The electrodes were set about 12 ± 1 mm apart and suspended near the flame. The current obtained was amplified with a current-to-voltage converter and then fed into a boxcar averager for signal processing. The result was displayed on an oscilloscope or stored in a microcomputer for later treatment of data.

FLAME TEMPERATURE

Measurement of the temperature of a flame is important in combustion chemistry. The methods used for this determination involve mostly optical spectroscopy in various ways, such as the line-reversal method, two-line method, laser-induced fluorescence, Raman spectrosopy, and Rayleigh scattering.[26,27] These approaches mostly rely upon an assumption of local thermal equilibrium, in which the flame temperature is represented in terms of electronic, vibrational, rotational, or translational behavior.

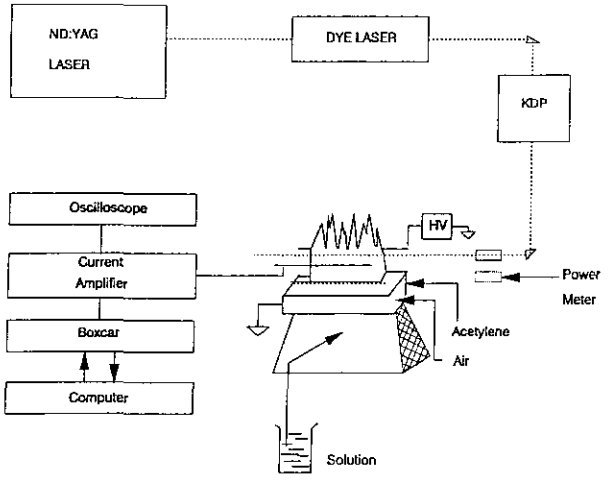

Fig. 1. Experimental setup for laser-enhanced ionization in a flame.

LEI has been employed to determine the diffusion and mobility coefficients associated with a flame.[14,15] In terms of these coefficients, the flame temperature has been estimated according to the Einstein relation.[15] As is the case for most methods, the temperature thus obtained is based on an assumption of local thermal equilibrium. The advantages of LEI lie in its capability to achieve great spatial resolution and to avoid effects of optical interference. Nevertheless, the inherent systematic error appears to be large, as a homogeneous electric field between two probing electrodes has to be assumed and the electrode dimensions and convection velocity are neglected.[15]

Instead of employing the Einstein relation, we developed a new version of the LEI technique to evaluate the flame temperature, based upon the Boltzmann population of the fine structure of the ground state of the species selected.[16] For a species with a fine-structure doublet in its ground state, the LEI response occurs through optical transitions and subsequent ionization. The optical excitation is conducted by either from the ground fine-structure level (l′) to an intermediate level (u) or from the excited fine-structure level (l) to the common intermediate level. According to a two-level approximation, an explicit and practical relation for the temperature measurement is[16]

$$T = (E_{l'} - E_l)/kQ \quad (1)$$

$$Q = \mathrm{Ln}(S_{ul} I_{\lambda'} \lambda^5_{ul'} A_{ul'} / S_{ul'} I_{\lambda} \lambda^5_{ul} A_{ul}). \quad (2)$$

in which $E_{l'}$ and E_l are the terms or energies of ground and excited fine structures of the species selected; k is the Boltzmann constant. S_{ul} and $S_{ul'}$ indicate the LEI signals, which result from the optical transitions $l \rightarrow u$ and $l' \rightarrow u$, respectively. I_λ and $I_{\lambda'}$ are the spectral irradiances at wavelengths λ and λ'.

If the spontaneous transition probablities A_{ul} and the corresponding transition wavelengths λ_{ul} for pertinent atomic transitions ($l \rightarrow u$) of an atom occurring in a flame are available from the literature, then by measuring the LEI signal of this atom and the power dependence of the LEI signal [i.e.(S_{ul}/I_λ)], one may obviously determine the flame temperature according to these equations.

A sample of Ga served as a test. The wavenumber difference between its fine structure states is 827 cm^{-1}; therefore the upper level can be thermally populated. An aqueous solution of the Ga salt was prepared at 100 ppm (μg/mL).

LEI detection of the Ga atom followed the procedure described in Sec. II. The ratio S_{ul}/I_{λ} was obtained from the measurement of the dependence of the Ga LEI signal on laser power. The resultant LEI measurements as a function of laser power for the transition $4^2P_{1/2} \rightarrow 4^2D_{3/2}$ or $4^2P_{3/2} \rightarrow 4^2D_{3/2}$, appear in Fig. 2. The laser power was maintained in the regime under saturation; hence the LEI signal of the Ga sample was ensured to be linearly proportional to the laser power. This condition is the criterion for valid application of Eqs. 1 and 2. In order to confirm that the derived model is applicable to any three-level system, we performed LEI measurements with excitation to various intermediate states of Ga analyte. The values 2504 ± 74 K and 2521 ± 31 K were thus obtained for two selected intermediate states $5^2S_{1/2}$ and $4^2D_{3/2}$, respectively. The excitations and associated transition probabilities are listed in Table 1. Accordingly, the satisfactory agreement with varied intermediate states indicates the success of the three-level model applied to measure the flame temperature.

To justify further that LEI is suitable to monitor flame temperature, pertinent measurements previously reported for the same air/acetylene flame are listed in Table 2. Temperature in the range 2400-2600 K were measured by optical spectroscopy, including atomic spectroscopy (AA),[28,29] atomic emission (AE),[28,30] and atomic fluorescence (AF).[31-33] Our measurements agree satisfactorily with those determined by other techniques, assuring that the determination of a flame temperature can be as reliable by means of LEI as by a well known optical method.

Table 1. Atomic Transitions and Relevant Spectral Data[44] of the Ga Element[a]

Element	Transition	λ(nm)	A($10^8 s^{-1}$)
Ga	$4^2P_{1/2} \rightarrow 5^2S_{1/2}$	403.298	0.49
	$4^2P_{3/2} \rightarrow 5^2S_{1/2}$	417.227	0.92
	$4^2P_{1/2} \rightarrow 4^2D_{3/2}$	287.465	1.2
	$4^2P_{3/2} \rightarrow 4^2D_{3/2}$	294.480	0.27

[a] λ and A represent the transition wavelength and the transition probability of each atomic transition, respectively. The uncertainty for the A value is 25%.

Relative to the LEI method based on the Einstein relation,[15] the model described here simplifies the evaluation of the flame temperature. To use the Einstein relation, one must measure the ion diffusion and ion mobility coefficients, a formidable task without the assumptions described above. In contrast, our version of LEI appears more convenient and more precise;[16] only two approximations — that of a steady state of the populated intermediate level and that of a Boltzmann distribution of populations of fine-structure states — are required. The steady state is a reasonable approximation, because the rate of excitation is small, under the condition of avoidance of saturation, but the rate of ionization of the excited atoms is large. As soon as the interme-

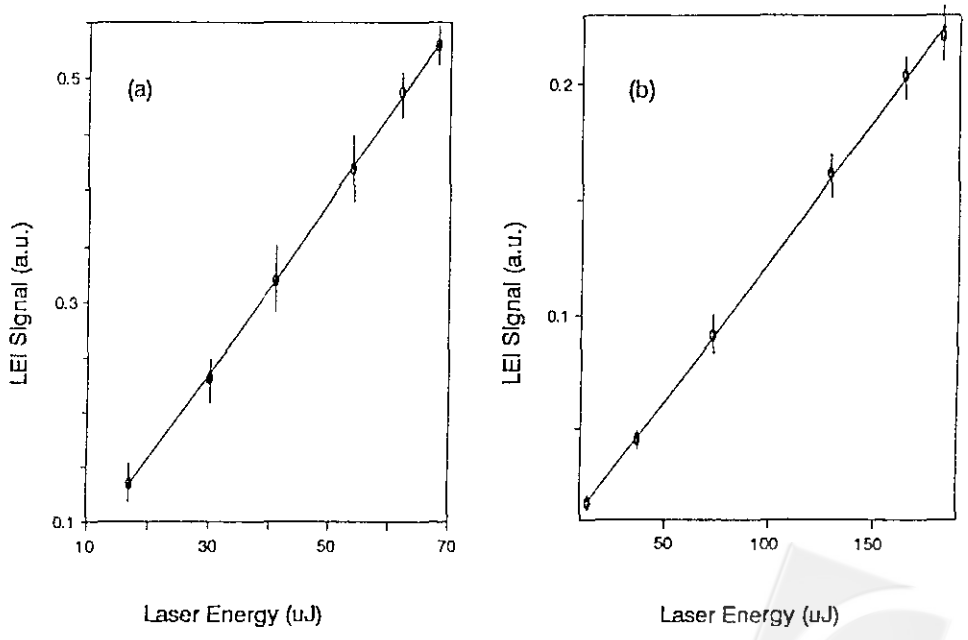

Fig. 2. Measurement of power dependence of laser-enhanced ionization signal due to Ga atomic transitions: (a) $4^2P_{1/2} \rightarrow 4^2D_{3/2}$ and (b) $4^2P_{3/2} \rightarrow 4^2D_{3/2}$.

Table 2. Flame Temperature of an Atmospheric Air/Acetylene Flame Determined by Using the LEI Method and Other Techniques

Method	A/F	H	Temperature (K)	Reference
LEI	12.5/0.5	7.5	2504±74, 2521±31	*This work*
AA	9.44/0.96	5.0	2450	28
AE	9.44/0.96	5.0	2460, 2480	28
AE	10.0/1.35	1.5 (4.5)	2430±35 (2420±25)	30
AF	9.8/1.5	2	2540±25	31
AA	9.5/1.3	4.5	2452, 2473	29
AF	8.25/1.15	32	2545±60, 2555±50	32
AF	7.6/1.04	3 (48)	2400 (2600)	33

AA, AE and AF in the first column represent atomic absorption spectroscopy, atomic emission spectroscopy and atomic fluorescence spectroscopy, respectively. The flow rates (in L/min) of air and fuel, denoted as A/F, and the measured position (in mm), denoted as H, from the burner head are separately listed in the second and third columns.

diate level is populated, it becomes depleted rapidly. This fact indicates that a steady state should be a valid approximation for the system.[3,34] The Boltzmann distribution is applicable to a flame in local thermal equilibrium, assumed in most methods.[15,35]

The demonstration with the Ga sample enables a conclusion. If an appropriate element is selected as analyte, provided that its two lowest atomic levels are close enough and that transition probabilities to one common upper level *are also available, the LEI technique can be a simple and* alternative way to determine the temperature of a flame.

ATOMIZATION EFFICIENCY

For analytical flame atomic spectrometry, various measurements of physical quantities are based on the number density of free atoms of an element in a flame. Thus the atomization efficiency[26,28,36-41] of elements being analyzed is a critical factor to govern the limit of detection. Previous measurements of this efficiency were performed only with atomic absorption[28,36-40] or atomic emission.[41]

We developed a useful scheme to apply LEI to determine the efficiency of atomization of metal elements in a flame.[13] In this scheme, rate equations for population densities at the relevant atomic energy levels and the relevant ionic state of an atom were solved. This approach yields a useful relation between the time-integrated LEI signal and the total number density of free atoms in a flame. We applied this relation to determine the atomization efficiency of lithium and sodium in an acetylene/air flame.

The atomization efficiency ε_a is defined as[26]

$$\varepsilon_a = n_a/n_t \tag{3}$$

in which n_a is the number density of free atoms of an element present in the flame, and n_t is the total number density of the same element actually nebulized.

To relate the response of LEI instrument to the number density of free atoms, one considers both the atomic transition and subsequent ionization.[3,16,42] Such a three-level system may be described in terms of rate equations, in which the time evolution of population density in each level is solved using Laplace transforms. Accordingly, the experimental time-integrated LEI signal is related to the number density n_a by the equation[13]

$$n_a = \frac{(x - y)}{Ge\sigma l\gamma z}\left[\frac{Q_e}{g_1} e^{E_1/kT}\right] \int_0^{\tau} V(t)\, dt \tag{4}$$

where

$$z = \{x[1 - \exp(-y\,\tau_l)] - y[1 - \exp(-x\,\tau_l)]\}$$

G represents the gain of the current amplifier, e the electron charge, σ the cross section between the laser beam and the flame, l the probing length, γ the collection efficiency, τ the integration interval, V(t) the amplified voltage pulse of the time-resolved LEI signal, τ_l the laser pulse duation, g_1 the degeneracy of atomic level 1 (normally equivalent to the ground state), E_1 the energy of atomic level 1, k the Boltzmann constant, and Q_e the atomic electronic partition function; x and y are the explicit functions of those rate coefficients considered in the three-level system, including Einstein A and B coefficients, and those for collisional ionization and collisional deactivation of the optically excited atoms.

The total number density n_t of the element in the flame is evaluated according to[41]

$$n_t = 2.98 \times 10^{21} \frac{C\Phi\varepsilon}{(n_T/n_{298})\, Tf} \tag{5}$$

in which C is the concentration (M) of the analyte solution, Φ the aspiration rate (mL/min), ε the efficiency of sample introduction, T the flame temperature, f the flow rate (mL/s) of unburnt gases at room temperature (298 K) and atmospheric pressure, n_{298} the quantity (mol) of species at room temperature, and n_T the quantity (mol) of combustion products at temperature T. If the Einstein A and B coefficients are available and the relevant rate coefficients are also given, one can determine the atomization efficiency of an element in the flame from time-resolved LEI measurement via Eqs. 3-5.

We describe here measurements of relevant parameters involved in the above equations. The analytes, lithium and sodium solutions, were prepared at several concentrations. With the formula of Chester et al.,[43] the term (n_T/n_{298}) in Eq. 5 was estimated to be 1.00 for the ratio acetylene : air = 1 : 25 and a flame temperature 2500 K. The aspiration rate was fixed at 4.5 cc/min. The efficiency of sample introduction ε was measured to be 0.088 ± 0.005. Using Eq. 5, we obtained the n_i value (3.14±0.08) × 10^{12}, (1.57±0.04) × 10^{12}, and (3.14±0.08) × 10^{11} mL^{-1} for lithium solutions of 10, 5, and 1 ppm (μg/mL), respectively, and (4.74±0.12) × 10^{11} mL^{-1} for a sodium solution of 5 ppm.[13]

The LEI current signal was probed either by a pair of stainless steel rod electrodes (length 20 mm and diameter 1.5 mm) or by a pair of stainless steel plate electrodes (20 × 16.5 × 0.5 mm^{-3}) along the laser beam. The probing volume was σl = 0.0628 mL. The detected current was first amplified with a calibrated gain factor G = (5.0±0.2) × 10^4 V/A. The resultant voltage pulse was then recorded on a digital oscilloscope and stored on microcomputer diskettes for later treatment of data. A measured time-resolved LEI voltage pulse due to the Li $2^2S_{1/2} \rightarrow 3^2P_J$ transition appears in Fig. 3.

The efficiency of ion collection γ was determined by a least-squares fit of the time-integrated LEI signal as a function of distance of the collection electrode from the center of the laser beam, where a unity ion collection efficiency was assumed. These plots for a 5-ppm sodium solution are presented in Fig. 4, in which the rod result was linearly fitted but the plate result only quadratically fitted. The LEI signal measured with the plate electrodes increased more than that with the rod electrodes as the collector was moved closer to the laser beam. The determined efficiency of ion collection were 0.48±0.03 (0.16±0.03) for a 10-ppm lithium solution, and 0.50±0.03 (0.13±0.02) for a 5-ppm sodium solution; the first numbers are the results for rod electrodes and the numbers in parentheses are results for plate electrodes.

Given the values of parameters as measured above, Einstein A and B coefficients,[44] and the relevant collision rate coefficients,[12,26,45-47] we evaluated the atomization efficiencies of lithium and sodium in terms of Eq. 3. The results are summarized in Table 3, in which previously reported values in an acetylene/air flame, analyte concentrations, flow rates of fuel and air, and flame temperatures are included for comparison. For lithium, the LEI results with the rod electrodes are consistent with those obtained with atomic absorption spectroscopy, but the results from the plate electrodes are slightly greater. Although the selected Li solutions are in the linear regime of LEI response, the at-

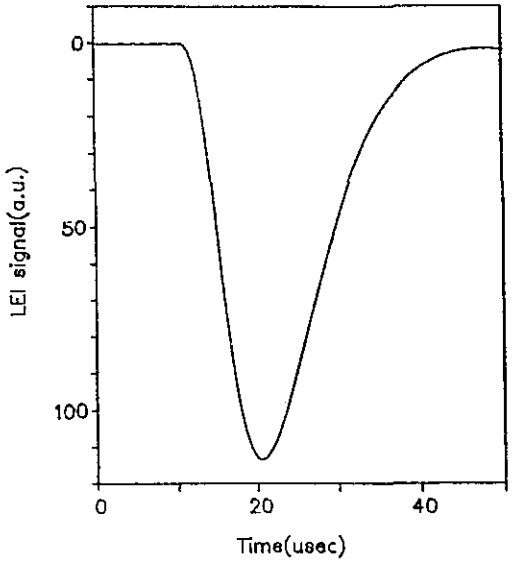

Fig. 3. A measured LEI voltage pulse due to the Li $2^2S_{1/2} \rightarrow 3^2P_J$ transition.

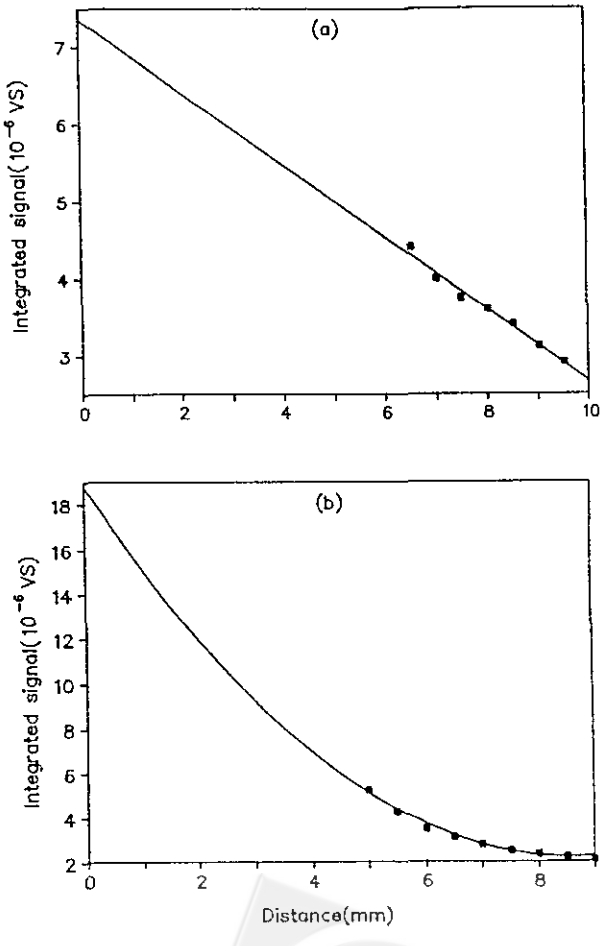

Fig. 4. Plots for the integrated LEI signal as a function of the distance of the collection electrode from the center of the laser beam: (a) for the result with rod electrodes, and (b) for the result with plate electrodes.

Table 3. Comparison between the Atomization Efficiencies ε_a Determined by the Time-integrated LEI Measurement and Those Reported by the AA Method for the Li and Na Elements in an Atmospheric Acetylene/Air Flame

Atom	ε_a	C[b]	F/A[b]	T[b]	Ref.
Li	0.13±0.02 (0.25±0.06)[a]	10	0.5/12.5	2500	This work
	0.14±0.02 (0.29±0.07)	5			
	0.16±0.02 (0.37±0.09)	1			
	0.21	-	0.7/7.56	2480	1
	0.20	32	1/5.6	2450	2
	0.12	16.7	0.96/9.44	2450	3*
Na	1.0±0.1 (1.0±0.2)	5	0.5/12.5	2500	This work
	1.00	-	0.7/7.56	2480	1
	0.50	0.1	1/5.6	2450	2
	0.52	16	1/5.6	2450	2
	1.00	0.05	1/5.6	2450	2*
	1.04	0.015	0.96/9.44	2450	3*

[a] The parenthesized values are the results from the plate electrodes.
[b] C is the concentration (in ppm) of the analyte solution, F/A denotes the flow rates (in L/min) of fuel and air, T represents the flame temperature (in K).
[1] From Ref. 48.
[2] From Ref. 40. *Measurement with 500 ppm Cs added.
[3] From Ref. 28. *Measurement with 1000 ppm Cs added.

omization efficiencies for the solutions of small Li concentrations (e.g. 1 ppm) appear slightly larger than those for the 10-ppm Li solution, especially with the plate electrodes. We attribute such a discrepancy to the fact that the assumption of uniform efficiency of ion collection for Li solutions of varied concentration may not be valid if there is interference from the effect of space charge. This interference could cause the collection efficiency determined for 10 ppm Li to be slightly smaller than its true value, and in turn cause the atomization efficiencies determined for the Li solutions of small concentrations to be slightly increased.

For sodium, LEI results from the rod and plate electrodes agree satisfactorily with each other, and with an AA value,[48] and with AA values determined with Cs added as a matrix element.[40,28] However our results are twice as large as those AA values determined without Cs added.[40] This significant discrepancy deserves further discussion, although a full explanation is impossible at present. Previous work revealed that the flame temperature, the matrix element added, and the ratio of fuel to oxidant play important roles with regard to the degree of atomization of a salt solution. According to the flame temperature of 2500 K in this work and 2450 K,[40] this discrepancy is unlikely due to the temperature factor. Given the flow rates of two flame gases, and the aspiration rate and introduction efficiency of the analyte solution of our work, the use of the Saha equation[35] provides an estimate of the number density of sodium ions (Na^+) that is only ~10% of that of free atoms of sodium. In our case, most sodium element may exist in the form of free atoms and, whereas half the sodium element in other experiments[40] may exist as ions and compounds. This argument is reasonable if we consider the ratios of acetylene to air 1:25 in our work and 1:5.6 elsewhere.[40] The latter flame is fuel-rich in which extra carbon-containing radicals can exist, affecting the atomization of sodium and explaining further why the effect of a Cs matrix plays an important role. Our value agrees satisfactorily with that[48] without matrix element added, in which the ratio of acetylene to air 1:10.8 is only about one half that in the other work.[40] These considerations indicate that the discrepancy is likely related to the varied composition of the flame. However, to understand fully the detailed mechanism behind this discrepancy, more work is definitely desirable.

According to these results on both lithium and sodium, we conclude that employment of LEI to determine the atomization efficiency of an element in a flame yield results comparable with AA measurements, provided that collisional quenching and collisional ionization rate coefficients are appropriately estimated.

ONE-STEP LEI VS TWO-STEP LEI

To improve the sensitivity and selectivity of LEI utilized in trace analysis, efforts have been made to treat electrical interference,[49-51] electrode design,[9,52] ion collection con-

figuration,[53,54] and influence of space charge and biased voltage on the ion collection efficiency.[55,56] Among these concerns, employment of two lasers through stepwise excitation, causing increased population of the analyte promoted to its higher states, has proved to be an efficient method to increase the ion yield.[1,3,57-60] The collisional ionization rate is thus expected to increase exponentially with decrease of energy difference between the populated state and the ionization continuum. As the LEI scheme with two-step excitation followed by collisional ionization is commonly used to detect trace analytes, it is important to characterize the ionization mechanisms and to compare the ion yields produced in single-step and two-step excitations.

One-step and two-step LEI mechanisms based upon the rate equations are thoroughly derived, relying upon several parameters related to rates of collisional ionization and quenching, transition probabilities and spectral irradiance of the laser.[42,60-63] With these parameters, the ion yields produced in two-step and one-step LEI processes may be effectively compared. Here we examine each individual parameter, which may cause enhancement of ion yield of two-step LEI relative to one-step LEI. The data are then compared to their theoretical counterpart, a simple model based upon the steady-state approximation, rough but suitable in practice to characterize the ion yield enhanced by two-step excitation.[6]

We consider the two-step LEI scheme as a system of four energy levels N_1-N_3 and N_i, of which excitation in the first-step transition is from N_1 to N_2, in the second-step from N_2 to N_3, and finally with collisional ionization from N_3 to N_i. To derive the ion yield for two-step LEI, we adopt three assumption. A steady-state approximation is applicable to the N_3 state; i.e. $dN_3/dt = 0$. The ion-electron recombination rate is small and negligible during the laser pulse duration 5-8 ns.[42] The laser profile is narrow like a delta function.

While the conditions of first-step excitation in both one-step and two-step LEI schemes are considered to be identical, either in optical saturation or in linear interaction with radiation, according to a complicated derivation, the ratio of N_i(TLEI) to N_i(SLEI) is[6,23]

$$R = \frac{N_i(TLEI)}{N_i(SLEI)} = \frac{\lambda_{23}^2 A_{32} I_{23} k_{3i}}{2\Pi\Delta\omega_{23} k_{2i}} \quad (6)$$

in which N_i(TLEI) and N_i(SLEI) indicate the ion yields induced by two-step and one-step LEI, respectively; k_{2i} and k_{3i} are the collisional ionization rate coefficiencies of the excited atoms from the N_2 and N_3 states; I_{23} denotes the laser intensity for the second-step excitation; λ_{23} is the wavelength for excitation from N_2 to N_3, A_{32}, the Einstein spontaneous emission coefficient, and $\Delta\omega_{23}$ the linewidth of the transition.

According to Eq. 6, the ion enhancement of TLEI over SLEI is attributed to the factors of second-step transition probability, laser intensity, collisional ionization rate coefficients, and transition linewidth, which is associated with the effective lifetime of the states involved in the transition. Eq. 6 is equivalent to Eq. 36 given by Axner et al.,[62] ignoring the possibility of atom depletion during the laser pulse. According to the latter model, with neglected atom depletion,[62] comparison of the ion enhancement between two-step LEI and one-step LEI becomes slightly dependent upon the power of first-step laser excitation, when the power of second-step laser excitation is adjusted to be weak. Although the factor of atom depletion generally influences the ion enhancement induced by two-step LEI, it can be made negligible by appropriate selection of the upper state of the second-step excitation, such that the duration of the laser pulse is less than the inverse of the rate of collisional ionization from this state.[62,63]

In order to examine those parameters related to the ion enhancement effect, we used K, Ca and Ba salts as reagents. Each aqueous salt solution (100 ppm) was nebulized at a flow rate 4.5 mL/min into the flame. The linearity of concentration dependence of LEI signal was verified. The energetic schemes of the two-step LEI process of K, Ca and Ba atoms are depicted in Fig. 5.

To examine the A_{32} dependence of ion yield enhanced by two-step LEI relative to one-step LEI process, we selected K as the reagent; the $4^2S_{1/2} \rightarrow 4^2P_{1/2}$ (or $4^2P_{3/2}$) transition was first excited, and then either the $4^2P_{1/2}$ (or $4^2P_{3/2}$) $\rightarrow$ $n^2S_{1/2}$ or $4^2P_{1/2}$ (or $4^2P_{3/2}$) $\rightarrow$ n^2D_J transition followed in the wavelength range 492-512 nm. A two-step LEI spectrum appears in Fig. 6, and the observed ion enhancement of TLEI/SLEI is presented in Table 4. Because the two-step

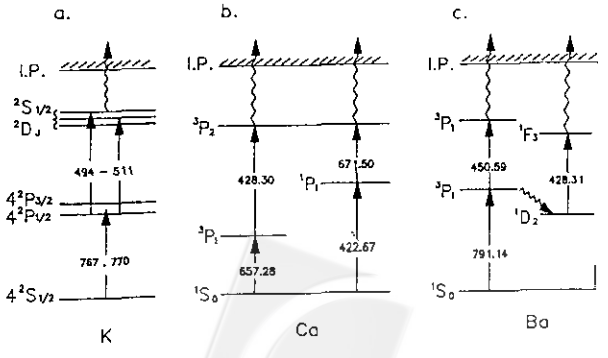

Fig. 5. Two-step LEI schemes for K, Ca and Ba atoms.

Table 4. Potassium Ion Enhancement of DLI/LEI[e]

Stepwise transition	State energy (cm^{-1})	Second-step wavelength (nm)	A_{32}[a] ($10^8 s^{-1}$)	n*[b]	μ[c]	Ion enhancement ExP[d]	Cal.
$4^2P_{1/2} \rightarrow 10^2S_{1/2}$	33214.4	494.20	0.00213	7.83	2.18	50	50
$4^2P_{3/2} \rightarrow 10^2S_{1/2}$	33214.4	495.61	0.00425	7.83	2.18	95	100
$4^2P_{1/2} \rightarrow 9^2S_{1/2}$	32648.2	508.43	0.00350	6.82	2.18	89	82
$4^2P_{3/2} \rightarrow 9^2S_{1/2}$	32648.2	509.92	0.00700	6.82	2.18	115	164
$4^2P_{1/2} \rightarrow 8^2D_{3/2}$	33178.4	495.08	0.00220	7.74	0.26	94	100
$4^2P_{3/2} \rightarrow 8^2D_{3/2,5/2}$	33178.4	496.50	0.0026	7.74	0.26	145	177
$4^2P_{1/2} \rightarrow 7^2D_{2/3}$	32598.5	509.72	0.0029	6.75	0.25	106	132
$4^2P_{3/2} \rightarrow 7^2D_{3/2,5/2}$	32598.5	511.22	0.0035	6.75	0.25	145	238

[a] Einstein spontaneous emission coefficient; see ref. 44.

[b] Defined as n-μ; n is the principal quantum number and μ is the quantum defect. Its value can be calculated by $1/\sqrt{\varepsilon}$; ε, in units of Rydberg, indicates the energy required to reach the ionization continuum.

[c] Quantum defect.

[d] Relative error = 10%.

[e] The calculated value is based on Eqs. 6 and 7 in the text, and then normalized to the experimental result for the trausition at $4^2P_{1/2} \rightarrow 10^2S_{1/2}$.

and one-step LEI schemes possess a common intermediate state, $4^2P_{1/2}$ (or $4^2P_{3/2}$), and because their conditions for first-step transition are identical, Eq. 6 may be employed to compare the yields of potassium ion in the two-step and one-step LEI processes.

In our experiment, the linewidth of each ionization profile resulting from the upper states, $n^2S_{1/2}$ or n^2D_J (Fig. 6) is roughly constant, the related wavelengths of second-step excitation lie within a small range, and the laser intensity is normalized. Therefore, the ratio of ion enhancement of TLEI/SLEI as a function of second-step excitation becomes simplified to[6]

$$\frac{R'}{R} \sim \frac{A_{32}'k_{3i}'}{A_{32}k_{3i}} \tag{7}$$

As these high-lying excited states are energetically near each other, the rates of collisional deactivation to the "neighborhood" states become so rapid[64,65] that the collisional ionization rates may be attributed to the summation of the ionization rates related to neighboring states. Therefore, we consider the ionization rates from these high-lying states to be roughly the same; i.e., $k_{3i}' \sim k_{3i}$. The relative ion enhancement of the various stepwise excitation is thus determined by the ratio of the corresponding second-step transition probability.

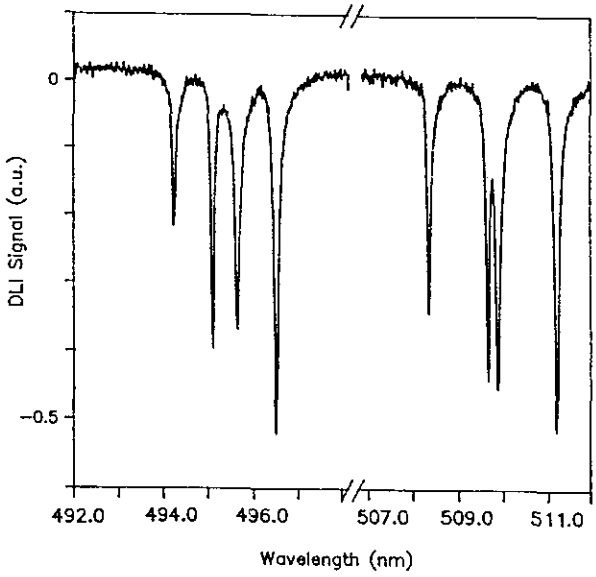

Fig. 6. Two-step LEI spectra for 100 ppm K atom in an acetylene/air flame. K atoms are excited first to the $4^2P_{1/2}$ (or $4^2P_{3/2}$) state, and then to either $n^2S_{1/2}$ (n=9,10) or n^2D_J (n=7,8) state.

To compare the experimental findings, we normalized the calculated ratio of TLEI/SLEI for the two-step LEI case with the second-step $4^2P_{1/2} \rightarrow 10^2S_{1/2}$ transition to its corresponding experimental value 50 ± 5. According to Eq. 7 and the assumption that $k_{3i}' \sim k_{3i}$, the ion enhancement related to various second-step transitions, $4^2P_{1/2} \rightarrow n^2S_{1/2}$ (n=9,10) or n^2D_J (n=7,8), agrees satisfactorily with our observation (Table 4).

The ratio of TLEI/SLEI through various first-step transitions is also predicted satisfactorily, except for cases involving the transition $4^2P_{3/2} \rightarrow 9^2S_{1/2}$ or $4^2P_{3/2} \rightarrow 7^2D_J$ as the second step. For instance, the ratio related to the $4^2P_{3/2} \rightarrow 10^2S_{1/2}$ transition is estimated to be 100, consistent with the observation 95 ± 10. To treat this case, we multiplied a fac-

tor of state-degeneracy ratio g_3/g_2 in the right-hand side of Eq. 6.[66]

Taking into account the degeneracy of states involved in the transitions and the respective first-step transition probability, we estimate the ratio TLEI/SLEI via the transition $4^2P_{3/2} \rightarrow 10^2S_{1/2}$ to be twice as large as that obtained via the transition $4^2P_{1/2} \rightarrow 10^2S_{1/2}$. Analogously, the ratios of TLEI/SLEI via the transitions $4^2P_{1/2} \rightarrow 8^2D_{3/2}$ and $4^2P_{3/2} \rightarrow 8^2D_J$ are estimated to be 100 and 177, in agreement with observed values 94 ± 10 and 145 ± 15, although the related A_{32} values appear to be almost equal.

The causes of the discrepancy from the model prediction may be complicated. As discussed above, the model is not perfect enough to account for the depletion of excited K atoms during the laser pulse. As a result, the ion enhancement of TLEI/SLEI may become dependent upon the power of the laser for the first-step excitation, which we neglected.[62,63] In addition, the Einstein spontaneous emission coefficient A_{32} reported bears an uncertainty 25 - 50%.[44] These considerations may partially explain the deviation observed in a comparison of ion enhancement results.

The Einstein spontaneous emission coefficient decreases with increasing the principal quantum number n. The transition probability is reported to be approximately proportional to $1/n^{*3}$.[67] n^* is the effective principal quantum number, equal to $n-\mu$ (μ is the quantum defect).[67] The A_{32} values listed in Table 4 agree with this prediction. Axner et al. demonstrated that the ionization signals of two-step LEI for Na, Li and Tl decrease with increased principal quantum number near the ionization continuum.[68] Therefore, an intuitive concept — that the state excited stepwise closer to the ionization continuum causes a larger ion enhancement — is untrue.

To examine the role of laser intensity in the secondfftep excitation, we selected Ca as the reagent. The two-step LEI scheme of Ca (Fig. 5b) is composed of a stepwise excitation via the transitions $4s^{21}S_0 \rightarrow 4s4p^3P_1$ and $4s4p^3P_1 \rightarrow 4p^{23}P_2$, whereas the one-step LEI scheme reflects only the transition $4s^{21}S_0 \rightarrow 4s4p^3P_1$. As the laser intensity in the first-step excitation is fixed, the ratio of two-step LEI to one-step LEI signal is measured as a function of laser intensity of the second-step excitation, and thereby shows a straight line of slope equal to unity. This result indicates that the second laser intensity in the two-step LEI scheme plays an important role in the optimization of the technique. According to Eq. 6, since the conditions of λ_{23}, A_{32}, k_{3i}, $\Delta\omega_{23}$ and k_{2i} parameters remain invariant, the ratio R becomes proportional to I_{23}. Our observation is consistent with the theoretical prediction. The result also indicates that the mechanism of collisional ionization is dominant over photoionization. In the latter process, the atoms populated in the upper state are ionized by absorbing an additional photon from either the first laser or the second laser. Using Na and Li as examples, Axner et al. in a comparison of the two-step LEI and photoionization techniques found that the former technique is several orders of magnitude more sensitive than the latter.[69]

We selected the Ca atom as a reagent to examine the influence of the factor k_{2i} upon ion enhancement by two-step LEI. As shown in Fig. 5b, two ionization schemes of the two-step LEI process of the Ca atom were used; one process involves the transition $4s^{21}S_0 \rightarrow 4s4p^3P_1$ at 657.3 nm as the first-step excitation and the transition $4s4p^3P_1 \rightarrow 4p^{23}P_2$ at 428.3 nm as the second-step excitation, whereas the other process is via the transition $4s^{21}S_0 \rightarrow 4s4p^1P_1$ at 422.7 nm and then the transition $4s4p^1P_1 \rightarrow 4p^{23}P_2$ at 671.5 nm. Both schemes possess a common upper state $4p^{23}P_2$. According to these schemes, the relative ion enhancement R′/R is rewritten as,[6]

$$\frac{R'}{R} = \frac{\lambda_{23}'^2 A_{32}' I_{23}'}{\lambda_{23}^2 A_{23} I_{23}} \exp\left[-(E_2-E_2')/kT\right] \qquad (8)$$

in which R′ and R indicate the ratio TLEI/SLEI for the processes $^1S_0$-$^3P_1$-$^3P_2$ and $^1S_0$-$^1P_1$-$^3P_2$, respectively. The "prime" notation indicates the process with the intermediate $^3P_1$ state involved.

Given (Table 5) published values of λ_{23}, A_{32}, λ_{23}', and A_{32}' as well as I_{23} and I_{23}' measured in our experiment, we estimate an R′/R ratio of 74, in agreement with our observation of relative ion enhancement 72 ± 12. This fact indicates that the ratio of ion yield of TLEI to SLEI may be enhanced when a small value of k_{2i} is selected. The two-step LEI technique may be performed more effectively for those species with a larger ionization continuum, from which a larger energy difference in the state excited leads to a smaller collisional ionization rate; thus the sensitivity of the one-step LEI scheme may be diminished. To increase the detection sensitivity of LEI with single-laser excitation, one should select an excited state close to the ionization continuum, provided that the transition probability remains reasonably large. Axner et al. adopted this strategy successfully to demonstrate the multielement-detection capability of one-step LEI using UV light as an excitation source for reducing the energy difference from the ionization continuum.[4]

Considering the specific nature of its intermediate state, we selected Ba atom as the reagent for the $\Delta\omega_{23}$ test. In the first two-step LEI scheme employed (Fig. 5c), the Ba atom was excited from the $6s^{21}S_0$ to the $6s6p^3P_1$ state at

Table 5. Experimental Measurement and Theoretical Calculation of Relative Ion Enhancement R′/R as a Function of Collisional Ionization Rate Coefficient and Transition Linewidth[a]

Element	First-step transition	Second-step transition	λ_1 (nm)	λ_2 (nm)	A_{32}[b] ($10^8 s^{-1}$)	I_{23} (μJ)	$(R'/R)_{exp}$	$(R'/R)_{cal}$
Ca	$4s^2{}^1S_0 \rightarrow 4s4p^3P_1$	$4s4p^3P_1 \rightarrow 4p^2{}^3P_2$	657.28	428.30	0.434	680±40		
							72±12	74
	$4s^2{}^1S_0 \rightarrow 4s4p^1P_1$	$4s4p^1P_1 \rightarrow 4p^2{}^3P_2$	422.67	671.50	1.4×10^{-5}	900±50		
Ba	$6s^2{}^1S_0 \rightarrow 6s6p^3P_1$	$6s6p^3P_1 \rightarrow 6p^2{}^3P_1$	791.14	450.59	1.1	430±30		
							0.98±0.28	0.4
	$6s^2{}^1S_0 \rightarrow 6s6p^3P_1$	$6s5d^1D_2 \rightarrow 6s4f^1F_3$	791.14	428.31	0.64	234±20		

[a] The parameters λ_1 and λ_2 indicate the first-step and the second-step transitions; A_{32} is the second-step Einstein spontaneous emission coefficient, and I_{23} is the second-step laser intensity. The calculated values of R′/R are based on Eqs. 8 and 9 in the text.

[b] see ref. 44; uncertainty within 25-50%.

791.1 nm, followed by absorption of a second photon to $6p^2{}^3P_1$ at 450.6 nm. In contrast, in the second two-step LEI scheme, the second laser was optically delayed by 2 ns with respect to the first laser and used to excite the transition $6s5d^1D_2 \rightarrow 6s4f^1F_3$ at 428.3 nm, whereas the transition of the first-step excitation was kept invariant. Comparing the relative ion enhancement of the first TLEI scheme with the second TLEI scheme, one obtains the following equation according to Eqs. 6 with correction of state degeneracy taken into account,

$$\frac{R'}{R} = \left(\frac{g_3' g_2}{g_2' g_3}\right) \frac{\lambda_{23}'^2 A_{32}' I_{23}' k_{3i}'}{\lambda_{23}^2 A_{32} I_{23} k_{3i}} \left(\frac{\Delta\omega_{23}}{\Delta w_{23}'}\right) \qquad (9)$$

Here R′ and R indicate the ratio of TLEI/SLEI induced by the first and second two-step LEI schemes, respectively. For making a quantitative comparison with experimental results, we adopted the following assumptions: $k_{3i}' \sim k_{3i}$, because the upper states $6p^2{}^3P_1$ and $6s4f^1F_3$ differ by less than 100 cm^{-1}; the population densities of the intermediate states $6s6p^3P_1$ and $6s5d^1D_2$ are assumed to be identical. Given the parameters in Table 5, in which $\Delta\omega_{23}/\Delta\omega_{23}'$ was measured to be 0.16 ± 0.03 and I_{23} and I_{23}' were 234 ± 20 μJ and 430 ± 30 μJ, respectively, we evaluate R′/R to be 0.4. Our observation of R′/R was 0.98 ± 0.28. Although the comparison seems to be in disagreement, the predicted value is expected to be smaller than that observed. Because there are several channels available to deplete the population of the intermediate state $6s6p^3P_1$, the population distributed to the $6s5d^1D_2$ state is expected to be less than that promoted initially. The R value of the second two-step LEI scheme is sensitive to the delay between these two laser pulses. As the delay was adjusted from 0 to 10 ns, the TLEI signal appeared to be at a maximum at 2 ns delay. Without knowledge of the branching ratio of the population partioning into the $6s5d^1D_2$ state, it is hard to estimate how much population remained in this state at 2 ns delay; therefore a precise quantitative comparison becomes impossible.

As demonstrated above, to optimize the two-step LEI configuration, the factors involving the second laser intensity, the transition probability of second-step excitation, the collisional ionization rates, and the transition linewidth (or quenching efficiency toward the excited states) should be taken into account. In our experiment, the findings are consistent with the model prediction, except for the effect of transition linewidth, which is underestimated theoretically due to the difficulty of establishing experimental conditions.

A TECHNIQUE TO DIMINISH ELECTRICAL INTERFERENCE

As LEI detects the species in an ionized form, the electrical interference inherent in this technique may diminish its sensitivity for trace detection. This interference results from such sources as ions and electrons produced in the flame background and easily ionized matrices mixed in the analytes. The effect of the interference upon the LEI technique is to reduce a signal-to-noise ratio and to hinder the applied electric field from reaching the radiation-interactive zone.

Study on electrical interference becomes crucial to improve the sensitivity of LEI for trace analysis. Methods applied to diminish this effect include sample pretreatment,[70,71] improvement of electrode design,[7,52,53] increase of biased voltage,[7,49,52,53] and employment of pulsed voltage-biased collectors.[54] These current methods, although effective to diminish electrical interference, may somehow cause such side effects as disturbance of the flame structure,[52] complication of the flame composition,[70] or lack of repro-

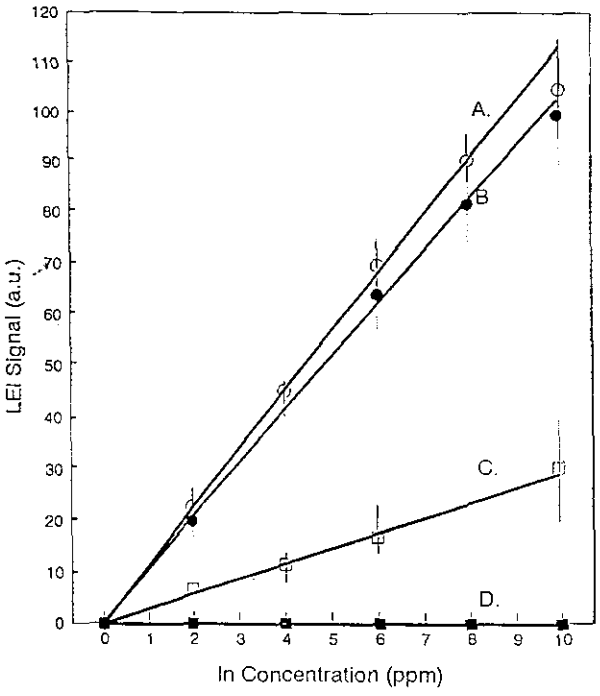

Fig. 7. Indium concentration dependence in conventional LEI detection in a solution with varied Na concentration added as the matrix. Curve A denotes the In solution without Na added, (o); B, 0.1 ppm Na added (•); C, 0.5 ppm Na added (□); D, 2 ppm Na added (■).

ducibility in LEI detection.[54]

In an effort to eliminate the electrical interference, we designed an apparatus by interfacing flow injection analysis (FIA) to the LEI device. In this way, the electrical interference was effectively reduced, and the linear dynamic range of sample concentration was much extended. The apparatus possesses advantages of good reproducibility and rapid sampling rates.[72]

In the following experiment, we use indium salt solution as the reagent and the sodium salt added as the matrix. The LEI signal of In is induced by optical excitation in the transition $5^2P_{3/2} — 5^2D_{5/2}$ followed by collisional ionization. The influence of the Na matrix upon the indium LEI intensity is shown in Fig. 7; the curves A, B, C, and D represent the indium concentration dependence of LEI detection in a 0.0, 0.1, 0.5 and 2 ppm Na solution, respectively. The LEI response appeared to be suppressed with increasing Na matrix. When the Na concentration was increased to 2 ppm, the indium LEI signal was suppressed completely, despite its concentration reaches as high as 10 ppm. (Fig. 7, curve D)

As the matrix concentration reached its threshold level at which no indium LEI signal was detected, with the use of our novel design of FIA-LEI apparatus, a significant LEI signal was resumed for detection. The design of the FIA-LEI apparatus is illustrated in Fig. 8. A single-channel FIA

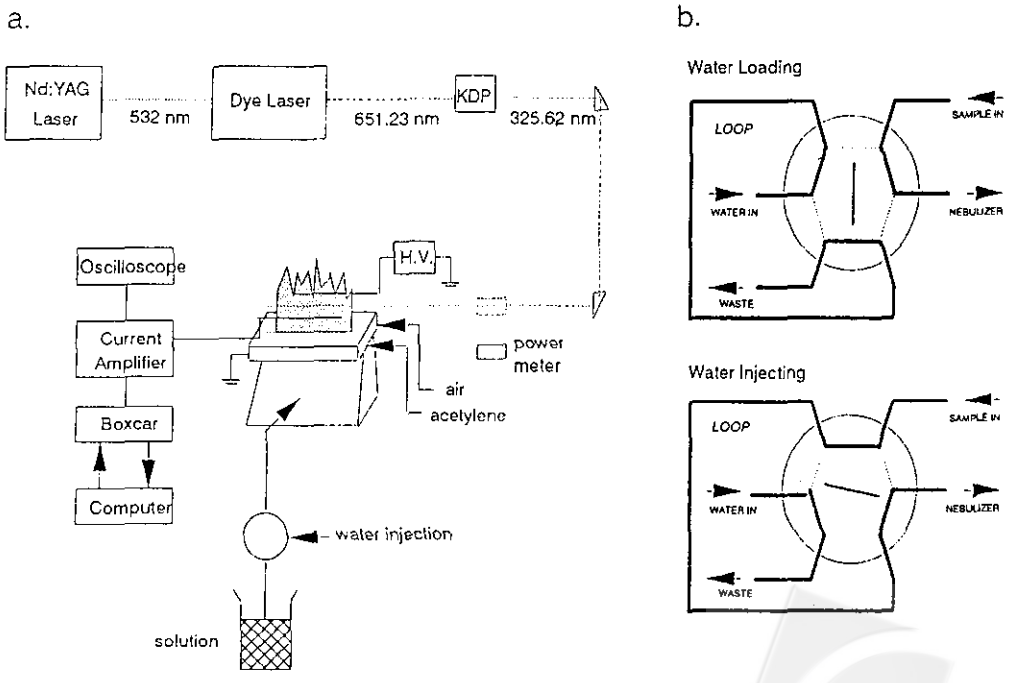

Fig. 8. (a) Schematic diagram of FIA-LEI apparatus. (b) A four-channel-based injection port. 1). Sample passes by the segment of distilled water loop; 2). As the valve is switched to release the distilled water in the loop, the segment of water flow is injected into the carrier stream of sample solution.

system was implemented to handle the solution prior to flowing towards the nebulizer. In this manner, a segment of distilled water flow was injected into the carrier stream of sample solution; the mixed solution was then nebulized into the flame in the same process as that without the FIA system involved. During the water loading, the sample flow with the original concentration was passed by this segment and continuously nebulized into the burner head. While the valve was switched to release the water in the loop, a 250 μL water zone was instantaneously dispersed into the carrier stream of the sample solution, causing dilution of the In sample to form a concentration gradient along the passage of flow. The water-injected mixture was transported towards the flame, in which the In atoms contained in the carrier stream were collisionally ionized following optical excitation to the $5^2D_{5/2}$ state. The operation procedure for FIA-LEI detection is otherwise the same as that in the so-called conventional LEI apparatus without implement of the FIA system.

Using the new FIA-LEI apparatus, we obtained a double-peak LEI signal, as shown in Fig. 9a, for a 4 ppm In solution mixed with 4 ppm Na as the matrix. To examine further whether the double peak is associated with the In sample, we tuned the laser slightly off resonance to wavelengths either 325.50 nm or 325.75 nm, and found that the LEI peak disappeared (Fig. 9b). As expected, the LEI signal also disappeared when a blank solution, composed of 4 ppm Na concentration alone, was irradiated with a laser beam at the resonance wavelength of 325.62 nm (Fig. 9c). As recalled from the preceding section, the conventional LEI device failed to detect any In trace when the Na matrix was increased to 2 ppm. A significant LEI signal was resumed in our FIA-LEI apparatus, which detected In in the solution containing Na concentration more than 40 ppm, about 20 fold that the conventional LEI apparatus can tolerate. The In concentration dependence of FIA-LEI detection in a 4, 8, 20, and 40 ppm Na solution, respectively, is shown in Fig. 10. The dynamic concentration dependence appeared linear

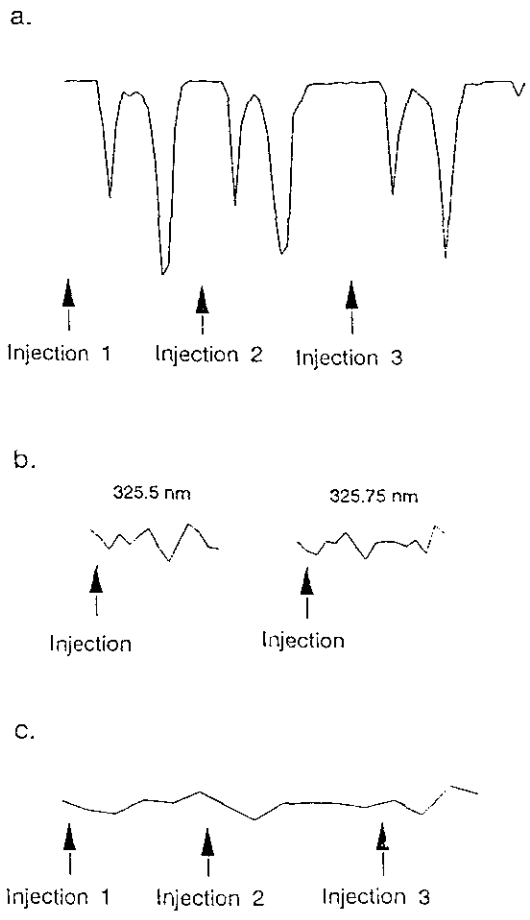

Fig. 9. (a) FIA-LEI detection of 8 ppm indium in a 4 ppm Na solution. A well defined volume of distilled water was injected in triplicate into a single-channel manifold of the FIA system. (b) The LEI signal disappeared as the laser was detuned to the wing wavelength either 325.50 nm or 325.75 nm. (c) No indium LEI signal was observed in a blank solution composed of 4 ppm Na alone, following optical excitation to the $5^2D_{5/2}$ state.

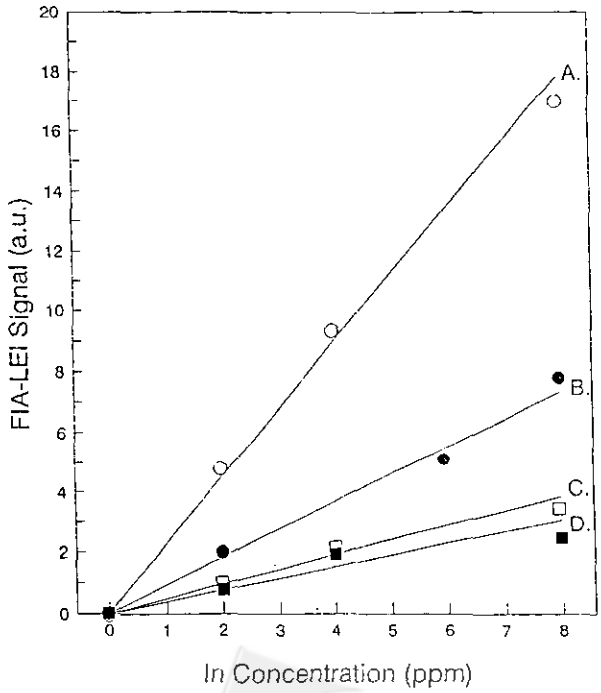

Fig. 10. FIA-LEI detection of the indium analyte in a mixture with varied concentration of Na: A. 4 ppm (o); B. 8 ppm (•); C. 20 ppm (□); D. 40 ppm (■).

within the In concentration studied; its slope tended to decrease with the Na concentration. Comparison of linear dynamic range of concentration between conventional LEI and FIA-LEI detection is shown in Fig. 11. Under otherwise identical experimental conditions, the linearity of In concentration dependence with the FIA-LEI detection in a 8 ppm Na solution can extend to a concentration of 30 ppm, about 6 fold that achieved in the conventional LEI apparatus.

Using the design of pulsed voltage-biased collectors, Nippoldt and Green[54] reported that a transient LEI signal of the In atom with K added as the matrix appears during the early period (a few hundred ms) before reaching the steady-state condition, in which the LEI signal is totally suppressed. Although the reproducibility of such a transient LEI signal is doubtful, the result indicates that in a matrix-interfering solution the LEI signal may penetrate through the resistance of electrical interference and become detectable, if some method is applied to disturb the homogeneous mixture from its equilibrium. The FIA technique is one such method, generally employed to generate a concentration gradient in the mixture of reagent and sample.[72] When a well defined volume of distilled water in the loop is injected into the sample carrier stream, the water dispersion through the solution makes the sample concentration dilute gradually to the extremity and then turn to condense along the passage of flow into the flame. Such a behavior of sample concentration gradient may explain the appearance of a double-peak LEI signal as shown in Fig. 9a. The early appearing small peak is caused by the gradually decreasing concentration of In, while the late, large peak comes from the gradually increasing concentration of In. The valley between the two peaks indicates lack of In sample in the central water zone.

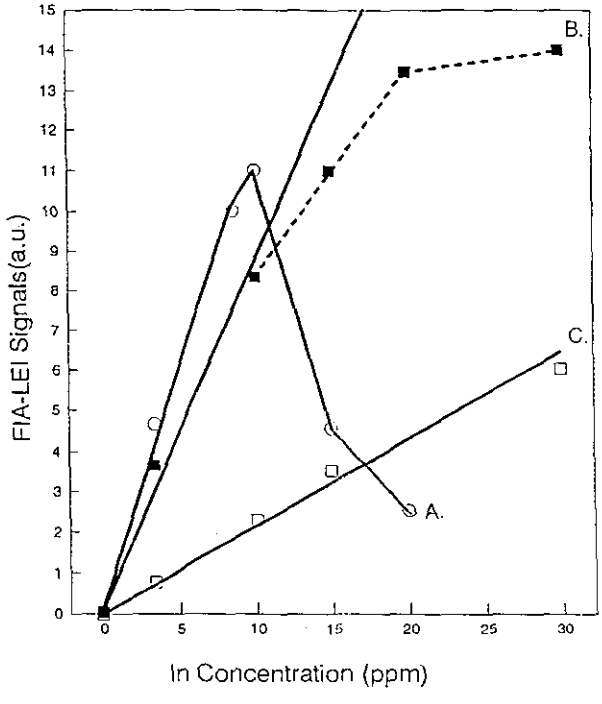

Fig. 11. LEI measurement as a function of In concentration. A. conventional LEI detection of the In sample in a solution without any Na matrix added. The intensity is scaled down by a factor of 0.25, (o); B. FIA-LEI detection of the In sample in a 4 ppm Na solution (■); C. FIA-LEI detection of the In sample in a 8 ppm Na solution (□).

The generated ions and electrons, while moving towards the opposite electrodes as a result of the applied electric field, produce a current for detection.[7,56,73] If the electric field is prevented from reaching the charged particles, then the produced current may diminish or even disappear. According to the theory of Lawton and Weinburg,[74] the shielding effect of the electric field caused by interference of those easily ionized species existing in the flame may be indicated by the ion sheath, which is formed due to the distinct mobility of ions and electrons such that a positive space charge is arround the cathode. The extent of ion sheath is associated with the ionization rates generated by the species in the flame; that is, the length of the ion sheath decreases with increasing the ionization rates of matrices. Under the steady-state approximation, the ionization rate becomes proportional to the matrix concentration. Accordingly, an increased matrix concentration may decrease the ion sheath by producing more ions and electrons. When the ion sheath is shorter than the distance between the cathode and the near-side edge of radiationinteractive regime, a finite electric field fails to reach the produced ions and electrons and then to separate these charged particles.[7,56,73,74] These particles without motion in the field result in a zero current. In view of this concept regarding the LEI detection, the generation of a concentration gradient in FIA is believed to help to dilute the matrix concentration, causing the ion sheath to become stretched out into the zone of charged particles. Such a diluting process is also at the expense of dilution of the sample. The resulting FIA-LEI intensity recovered is diminished to some extent, relative to the conventional LEI signal under an interference-free condition.

FIA-LEI detection possesses another remarkable advantage, having a much greater range of linear dependence of sample concentration than that achieved in the conventional LEI technique. For instance, Fig. 11 reveals that the linearity of In concentration dependence measured in the

conventional LEI method is restricted within 5 ppm, whereas that can extend to 30 ppm (or 10 ppm) with a mixture of 8 ppm (or 4 ppm) Na by means of the FIA-LEI apparatus. It is worthwhile to understand qualitatively the dynamic behavior of concentration in the new apparatus with respect to conventional LEI. In the latter measurement, the deviation from linearity of the In concentration dependence is attributed mainly to the space charge, which causes shielding of the electric field.[7,56,73] The more the charged particles are formed in the flame, the more significant the space charge effect may become. The influence of the space charge increases with the In concentration; this consideration may explain why the detected LEI intensity levels off and then tends to decrease with the In concentration. In the FIA-LEI apparatus, the concentrations of In and Na are simultaneously diluted, such that a finite electric field may interact with the radiation-active zone. The character of the dilution gradient leads to decreased total ion density in the flame, and thereby the space charge is much diminished. Accordingly, the linear range extends to a greater concentration of indium before deviation from the linear relationship. As the measured FIA-LEI signal of In is linearly proportional to its concentration, we can apply the standard addition method to recover its true concentration. However, the precision of recovery of the original analyte concentration is less reliable with increasing suppression effect of Na matrix.

In summary, our design of FIA-LEI apparatus can be a successful technique, capable of detecting a trace sample from an environment with severe matrix interference, thereby leading to resumption of the standard addition method. It can also be integrated with methods applied previously to make efficient use of this new technique.

CONCLUSION

From various applications of LEI demonstrated in the paper, we believe that LEI has matured to become a powerful analytical tool, not only for trace detection but also in many other prospects. To open new fields of LEI exploration, in addition to the analytical instrument itself, the development of an appropriate model seems crucial to relate significantly the observed LEI instrument response to those physical quantities involved in the system.

ACKNOWLEDGMENT

The author wishes to thank his co-workers for making this paper a reality and the National Science Council of the Republic of China for financial support (contract no. NSC82-0115-M001-170).

Received February 3, 1994.

Key Words

Laser-enhanced ionization; Flame temperature; Atomization efficiency; Flow-injection analysis.

REFERENCES

1. Travis, J. C.; Turk, G. C.; Green, R. B. *Anal. Chem.* **1982**, *54*, 1006A.
2. Axner, O.; Lindgren, I.; Magnusson, I.; Rubinsztein-Dunlop, H. *Anal. Chem.* **1985**, *57*, 773.
3. Omenetto, N.; Berthoud, Th.; Cavalli, P.; Rossi, G. *Anal. Chem.* **1985**, *57*, 1256.
4. Axner, O.; Magnusson, I.; Peterson, J.; Sjostrom, S. *Appl. Spectrosc.* **1987**, *41*, 19.
5. van Dijk, C. A.; Curran, F. M.; Lin, K. C.; Crouch, S. R. *Anal. Chem.* **1981**, *53*, 1275.
6. Su, K. D.; Lin, K. C. *Appl. Spectrosc.* **1994**, *48*, 241.
7. Turk, G. C.; Travis, J. C.; DeVoe, J. R.; O'Haver, T. C. *Anal. Chem.* **1979**, *51*, 1890.
8. Turk, G. C.; DeVoe, J. R.; Travis, J. C. *Anal. Chem.* **1982**, *54*, 643.
9. Cool, T. A. *Appl. Optics* **1984**, *23*, 1559.
10. Berglind, T.; Nillson, S.; Rubinsztein-Dunlop, H. *Phys. Scripta* **1987**, *36*, 246.
11. Turk, G. C.; Omenetto, N. *Appl. Spectrosc.* **1986**, *40*, 1085.
12. Smith, B. S.; Hart, L.; Omenetto, N. *Anal. Chem.* **1986**, *58*, 2147.
13. Su, K. D.; Lin, K. C.; Luh, W. T. *Appl. Spectrosc.* **1992**, *46*, 1370.
14. Mallard, E. G.; Smyth, K. C. *Comb. Flame* **1982**, *44*, 61.
15. Lin, K. C.; Hunt, P. M.; Crouch, S. R. *Chem. Phys. Lett.* **1982**, *90*, 111.
16. Su, K. D.; Chen, C. Y.; Lin, K. C.; Luh, W. T. *Appl. Spectrosc.* **1991**, *45*, 1340.
17. Mallard, W. G.; Houston, J.; Smyth, K. C. *J. Chem. Phys.* **1982**, *76*, 3483.
18. Axner, O.; Berglind, T. *Appl. Spectrosc.* **1986**, *40*, 1224.
19. Cool, T. A.; Tjossem, P. J. H. in *Gas-Phase Chemiluminescence and Chemi-ionization*; Fontijn, A., Ed.; Elsevier Science Publishers: Amsterdam, North-Holland, **1985**.

20. Cool, T. A.; Goldsmith, J. E. M. *Appl. Optics* **1987**, *26*, 3542.
21. Epler, K. S.; O'Haver, T. C.; Turk, G. C.; MacCrehan, W. A. *Anal. Chem.* **1988**, *60*, 2062.
22. Wang, S. C.; Lin, K. C. *Anal. Chem.* **1994** (in press).
23. Lin, K. C.; Duh, Y. S. *Appl. Spectrosc.* **1989**, *43*, 20.
24. Lin, K. C.; Duh, Y. S.; Sheu, T. C.; Hsu, T. J. *J. Chin. Chem. Soc.* **1988**, *35*, 179.
25. Axner, O.; Sjostrom, S. *Appl. Spectrosc.* **1990**, *44*, 864.
26. Alkemade, C. Th. J.; Hollander, T.; Snelleman, W.; Zeegers, P. J. Th. *Metal Vapors in Flames*; Pergamon Press: New York, **1982**.
27. Crosley, D. R. *Laser Probes for Combustion Chemistry*; ACS Symp. Ser. No. 134; American Chemical Society: Washington, D.C., **1980**.
28. DeGalan, L.; Samaey, G. F. *Spectrochim. Acta* **1970**, *25B*, 245.
29. Browner, R. F.; Winefordner, J. D. *Anal. Chem.* **1972**, *44*, 247.
30. Kirkbright, G. F.; Sargent, M.; Vetler, *Spectrochim. Acta* **1970**, *25B*, 465.
31. Omenetto, M.; Benetti, D.; Rossi, G. *Spectrochim. Acta* **1972**, *27B*, 453.
32. Haraguchi, H.; Smith, B.; Weeks, S.; Johnson, D. J.; Winefordner, J. D. *Appl. Spectrosc.* **1977**, *31*, 156.
33. Haraguchi, H.; Winefordner, J. D. *Appl. Spectrosc.* **1977**, *31*, 195.
34. Volk, L.; Richardson, W.; Lau, K. H.; Lin, S. H. *J. Chem. Educ.* **1977**, *54*, 95.
35. Gaydon, A. G.; Wolfhand, H. G. *Flame: Their Structure, Radiation and Temperature*; Chapman and Hall: London, **1979**; 4th ed.
36. Pupyshev, A. A.; Moskalenko, N. I.; Muzgin, V. N; Shalkauskas, Yu. S. *J. Anal. Chem. USSR* **1991**, *45*, 1641.
37. Osipova, V. A.; Kuzyakov, Yu. Ya.; Semenenko, K. A.; Gorlova, M. N. *J. Anal. Chem. USSR* **1985**, *40*, 630.
38. Kozyreva, G. V.; Shcherbakova, S. L.; Kuzyakov, Yu. Ya. *J. Anal. Chem. USSR* **1982**, *37*, 916.
39. Zeegers, P. J. Th.; Townsend, W. P.; Winefordner, J. D. *Spectrochim. Acta* **1969**, *24B*, 243.
40. de Galan, L.; Winefordner, J. D. *J. Quant. Spectrosc. Radiat. Transfer* **1967**, *7*, 251.
41. Winefordner, J. D.; Vickers, T. *J. Anal. Chem.* **1964**, *36*, 1939.
42. Omenetto, N.; Smith, B. W.; Hart, L. P. *Fresenius Z. Anal. Chem.* **1986**, *324*, 683.
43. Chester, J. E.; Dagnall, R. M.; Taylor, M. R. G. *Anal. Chim. Acta* **1970**, *51*, 95.
44. Wiese, W. L.; Martin, G. A. in *Wavelengths and Transition Probabilities for Atoms and Atom Ions*, Part II; NSRDS-NBS 68, **1980**.
45. Jenkins, D. R. *Proc. Roy. Soc.* **1968**, *A 306*, 413.
46. Gallagher, T. F.; Cooke, W. E.; Edelstein, S. A. *Phys. Rev.* **1978**, *A 17*, 125.
47. Smyth, K. C.; Schenck, P. K.; Mallard, W. G. in *Laser Probes for Combustion Chemistry*; ACS Symp. Ser. No. 134; Crosley, D. R., Ed.; American Chemical Society: Washington, D.C. **1980**.
48. Hinnov, E.; Kohn, H. *J. Opt. Osc. Am.* **1957**, *47*, 156.
49. Green, R. B.; Havrilla, G. J.; Trask, T. O. *Appl. Spectrosc.* **1980**, *34*, 561.
50. Havrilla, G. J.; Carter, C. C. *Appl. Optics* **1987**, *26*, 3510.
51. Axner, O.; Berglind, T.; Heully, J. I.; Lingren, I.; Rubinsztein-Dunlop, H. *J. Appl. Phys.* **1984**, *55*, 3215.
52. Turk, G. C. *Anal. Chem.* **1981**, *53*, 1187.
53. Havrilla, G. J.; Green, R. B. *Anal. Chem.* **1980**, *52*, 2376.
54. Nippoldt, M. A.; Green, R. B. *Anal. Chem.* **1983**, *55*, 554.
55. Havrilla, G. J.; Schenck, P. K.; Travis, J. C.; Turk, G. C. *Anal. Chem.* **1984**, *56*, 186.
56. Turk, G. C. *Anal. Chem.* **1992**, *64*, 1836.
57. Curran, F. M.; Lin, K. C.; Leroi, G. E.; Hunt, P. M.; Crouch, S. R. *Anal. Chem.* **1983**, *55*, 238.
58. Magnusson, I.; Axner, O.; Rubinsztein-Dunlop, H. *Phys. Scripta* **1986**, *33*, 429.
59. Turk, G. C. *Anal. Chem.* **1991**, *63*, 1607.
60. Lin, K. C.; Lin, S. H.; Hunt, P. M.; Leroi, G. E.; Crouch, S. R. *Appl. Spectrosc.* **1989**, *43*, 68.
61. Axner, O.; Berglind, T.; Heully, J. L.; Lindgren, I.; Rubinsztein-Dunlop, H. *J. Appl. Phys.* **1984**, *55*, 3215.
62. Axner, O.; Norberg, M.; Rubinsztein-Dunlop, H. *Spectrochimica Acta* **1989**, *44B*, 693.
63. Axner, O.; Rubinsztein-Dunlop, H. *Spectrochimica Acta* **1989**, *44B*, 837.
64. Luo, Y. L.; Lin, K. C.; Liu, D. K.; Luh, W. T. *Phys. Rev.* **1992**, *A 46*, 3834.
65. Chang, H. C.; Luo, Y. L.; Lin, K. C. *J. Chem. Phys.* **1991**, *94*, 3529.
66. Letokhov, V. S. *Nonlinear Laser Chemistry*; Springer-Verlag: Berlin, **1983**; Chap. 3.
67. Fabre, C.; Haroche, S. in *Rydberg States of Atoms and Molecules*; Stebbings, R. F.; Dunning, F. B., Eds.; Cambridge University Press: London, **1983**.
68. Axner, O.; Berglind, T.; Sjostrom, S. *Phys. Scripta* **1986**, *34*, 18.
69. Axner, O.; Sjostrom, S. *Appl. Spectrosc.* **1990**, *44*, 144.

70. Trask, T. O.; Green, R. B. *Anal. Chem.* **1981**, *53*, 320.
71. Bykov, I. V.; Chekalin, N. V.; Tikhomirova, E. I. *J. Anal. Chem.* (*USSR, Eng. Trans.*) **1986**, *40*, 1579.
72. Ruzicka, J.; Hansen, E. H. *Flow Injection Analysis*; John Wiley & Sons: New York, **1988**; 2nd edition; Chap. 1-4.
73. Schenck, P. K.; Travis, J. C.; Turk, G. C.; O'Haver, T. C. *J. Phys. Chem.* **1981**, *85*, 2547.
74. Lawton, J.; Weinberg, F. J. *Electrical Aspects of Combustion*; Clarendon Press: Oxford, **1969**; Chap. 8.